# Characterization of Magnetic Ultrathin Films by Novel Spectroscopic Methods

**Department of Materials Molecular Science**
**Division of Electronic Structure**

| | |
|---|---|
| YOKOYAMA, Toshihiko | Professor |
| NAKAGAWA, Takeshi | Assistant Professor |
| TAKAGI, Yasumasa | Assistant Professor |
| EGUCHI, Keitaro | Graduate Student |
| FUNAKI, Yumiko | Secretary |
| IWATA, Yumi | Secretary |
| KOSHIMIZU, Junko | Secretary |


Novel properties of magnetic metal ultrathin films have been attractive both from fundamental interest and from technological requirements. We are especially interested in drastic modification of metal thin films by surface chemical treatment such as adsorption-induced spin transitions and morphological changes. The magnetic properties are characterized by means of several kinds of spectroscopic methods like MOKE (Magneto-Optical Kerr Effect) using UV-visible lasers and XMCD (X-ray Magnetic Circular Dichroism) using synchrotron radiation soft X-rays.

Moreover, we have been exploiting new techniques based on UV photoemission magnetic circular dichroism (MCD) such as ultrafast time resolved UV MCD photoelectron emission microscopy (PEEM) for spatiotemporal magnetic imaging.

## 1. Growth Process and Magnetic Properties of Fe Nanoparticles Deposited on $Si_3N_4$/Si(111)-(8×8)

The magnetic properties of ferromagnetic transition metals on Si substrates have been widely investigated for the exploitation of new magnetic devices. Since clean Si surfaces react with transition metals very easily to form usually non-magnetic transition-metal silicides, it is essential to insert some inert film between transition metals and Si substrate. No reports have been however published for epitaxially ordered substrates on Si(111). In the present study, we investigated growth processes and magnetic properties of Fe deposited on well-defined $Si_3N_4$/Si(111)-(8×8), by using STM and XMCD.

Figures 1(a) and 1(b) show the STM images of the $Si_3N_4$/Si(111)-(8×8) substrate surface and 7.5 ML (monolayer) Fe deposited on the substrate. The substrate surface exhibits clear (8×8) superstructure that was also verified by LEED (low energy electron diffraction). The 7.5 ML Fe film shows the formation of Fe nanoparticles with the average diameter of ~6.9 nm. Figure 1(c) shows the Fe *L*-edge XMCD spectra of Fe deposited on $Si_3N_4$/Si(111)-(8×8) and clean Si(111)-(7×7). It is clearly found that the XMCD signals of Fe/$Si_3N_4$ are much larger than those of Fe/Si(111), especially for small Fe coverages. Figure 2(d) shows the magnetization curves of 1.6

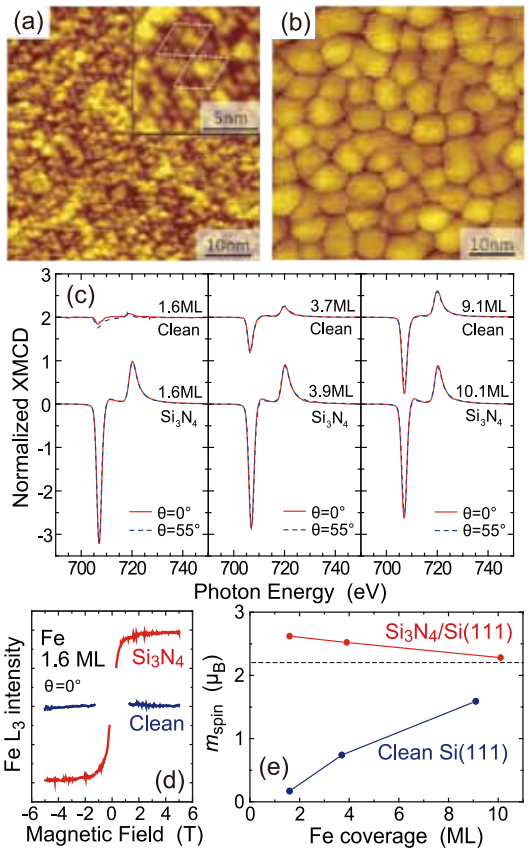


**Figure 1.** (a,b) 55×55nm$^2$ STM images of (a) $Si_3N_4$/Si(111)-(8×8) substrate and (b) the 7.5 ML Fe deposited film on the substrate. (c) Fe $L_{3,2}$-edge XMCD of Fe on clean Si(111) and $Si_3N_4$ at $\mu_0 H$ = ±5 T and $T$ = 5 K. The X-ray incidence angles θ are 0° (normal incidence) and 55° (grazing). (d) Magnetization curves of 1.6 ML Fe on clean Si(111) (blue) and $Si_3N_4$ (red), taken at $T$ = 5 K and θ = 0° by fixing the photon energy at the $L_3$ peak top. (e) Spin magnetic moments $m_{spin}$ of Fe on clean Si(111) (blue) and $Si_3N_4$ (red) at $T$ = 5 K as a function of Fe coverage.

ML Fe on the two substrates, again exemplifying a large and almost no magnetization of Fe on $Si_3N_4$ and clean Si(111), respectively. The XMCD spectra in Figure 1(c) allow us to obtain spin and orbital magnetic moments by using the so-called sum rules. The results are given in Figure 1(e). On clean Si(111)-(7×7), the spin magnetic moment is very small at low coverage and is enhanced with the increase in Fe coverage. On the contrary, Fe/$Si_3N_4$ has a much larger spin magnetic moment of 2.62 $\mu_B$, which is even larger than that of bcc bulk Fe (2.2 $\mu_B$). Such a drastic difference between the clean Si and $Si_3N_4$ substrates is caused by the fact that the $Si_3N_4$ substrate effectively suppresses the silicide formation. Because of the weak interaction with the $Si_3N_4$ substrate and the mismatch of the lattice constant, Fe/$Si_3N_4$ grows as nanoparticles that exhibit superparamagnetism. A larger spin magnetic moment at small Fe coverage is attributed to the size effect; the reduction of the particle size enhances the ratio of surface atoms that may exhibit larger magnetic moments.

## 2. Anharmonicity and Quantum Effects in Thermal Expansion of an Invar Alloy[1)]

Anomalously small thermal expansion over a wide temperature range in an iron-nickel alloy with a nickel concentration of around 35% was discovered by Guillaume in 1897, who was awarded the Nobel Prize in Physics in 1920. The effect is well known as the Invar effect and has been utilized in various kinds of industrial products. It has been recognized that the effect originates from magnetism. A basic concept of the Invar effect is that there exist at least two types of electronic states in Fe, typically high-spin (HS) and low-spin (LS) states. In this two-state model, the equilibrium potential energy is lower in the HS state than in the LS one, while the equilibrium atomic radius is larger in the former. This results in the compensation of thermal expansion due to increasing density of the LS state at higher temperature. Computational simulations at finite temperatures have also been carried out for the understanding of magnetization and thermal expansion. There have been, however, no reports concerning quantum-mechanical dynamics calculations, such as path-integral Monte Carlo (MC) simulations, although in general thermal expansion inherently results from anharmonic vibration, to which the quantum effect is essentially important at low temperature. In this work, we have investigated the anharmonicity and quantum effects in the Invar alloy $Fe_{64.6}Ni_{35.4}$. We have performed Fe and Ni *K*-edge extended x-ray-absorption fine-structure (EXAFS) spectroscopic measurements and the computational simulations based on the path-integral effective-classical-potential (PIECP) theory.

Figure 2(a) show the cohesive energies of hypothetical *fcc* Fe and the Invar alloy as a function of the lattice distance. In the present atomic potentials, fcc Fe shows that the LS state is more stable by 8.0 meV than the HS state, while the Invar case exhibits a more stable HS state by 25.0 meV. The bond distances of the HS and LS states are around $R_{HS}$ = 2.530 Å and $R_{LS}$ = 2.490 Å, respectively. Figures 2(b) and 2(c) show the first nearest-neighbor (NN) shells around Fe and Ni, respectively. Those around Fe show almost no thermal expansion, while those around Ni exhibit meaningful but smaller expansion than that of fcc Ni. At low temperature (< 100 K), the quantum effect is found to play an essentially important role. This is confirmed by comparing the quantum-mechanical simulations to the classical ones, the latter of which exhibit large (normal) thermal expansion at low temperature.

It is also revealed that thermal expansion for the Ni–Ni and Ni–Fe pairs is noticeably suppressed, even though the Ni electronic state may not vary depending on the temperature. On the other hand, the anharmonicity (asymmetric distribution) clearly exists for all the first NN shells as in the case of the normal thermal expansion system, where thermal expansion originates almost exclusively from the anharmonic interatomic potential. This implies the breakdown of the direct correspondence between thermal expansion and anharmonicity in a simple two-body model.

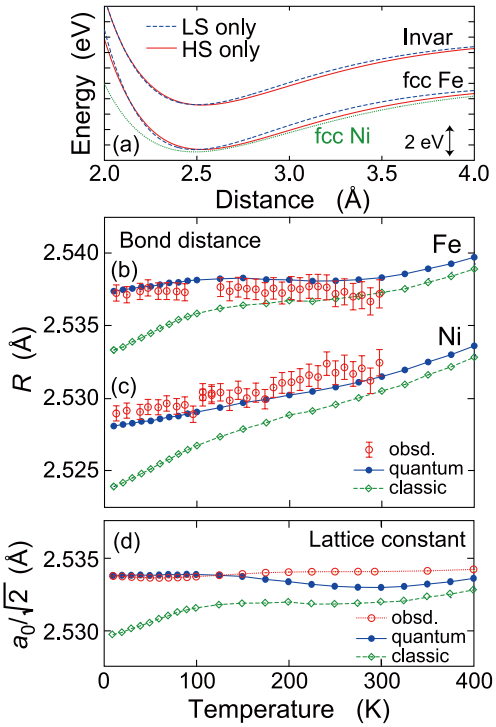


**Figure 2.** (a) Cohesive energies of Invar $Fe_{64.6}Ni_{35.4}$ (top lines), *fcc* Fe (bottom lines), and *fcc* Ni (bottom, green dotted line) as a function of the 1st NN distance at a temperature of 0 K. For Fe, two types of the potentials for the HS (red solid line) and LS (blue dashed line) states are depicted. (b),(c) Simulated 1st NN bond distance around Fe (b) and Ni (c) given by the PIECP (blue circles and solid line, quantum) and the classical MC (green diamond and dashed line, classic) methods, together with the experimental EXAFS data (red open circle with an error bar). (d) Equilibrium 1st NN distance ($a_0/\sqrt{2}$) given by the PIECP and classical MC simulations, together with the experimental literature data (red circle and dotted line).

### Reference

1) T. Yokoyama and K. Eguchi, *Phys. Rev. Lett.* **107**, 065901 (2011).